DETERMINING VITREOUSNESS OF DURUM WHEAT USING TRANSMITTED AND REFLECTED IMAGES

N. Wang, N. Zhang, F. E. Dowell, T. Pearson

ABSTRACT. *Digital imaging technology has found many applications in the grain industry. In this study, images of durum wheat kernels acquired under three illumination conditions (reflected, side−transmitted, and transmitted) were used to develop artificial neural network models to classify durum wheat kernels by their vitreousness. The results showed that the models trained using transmitted images provided the best classification for the nonvitreousness class (100% for non−vitreous kernels and 92.6% for mottled kernels). Results of the study also indicated that using transmitted illumination may greatly reduce the hardware and software requirements for the inspection system, while providing faster and more accurate results for inspection of vitreousness of durum wheat.*

Keywords. *Automation, Grading, Illumination, Inspection, Machine vision, Wheat.*

As a major class of wheat, durum (*Triticum turgidum* L. var. durum) production accounts for approximately 8% of the wheat production worldwide (Abaye et al., 1997). Durum wheat is mainly used to make semolina for macaroni, spaghetti, and other pasta products. The best durum wheat for pasta products should appear hard, glassy, and translucent, and have excellent amber color, good cooking quality, and high protein content. Nonvitreous (starchy) kernels are opaque and softer, and result in decreased yield of coarse semolina. Thus, vitreousness of durum wheat has been used as one of the major quality attributes in grading.

Traditionally, grain grading has been primarily done by visual inspection by trained personnel. This method is subjective and tedious. It also produces great variations in inspection results between inspectors. Targeting the disadvantages of human inspection, much research has been conducted to develop objective, rapid, and automated grain−grading systems.

Vitreousness is the nature of an object that resembles glass in transparency, brittleness, hardness, and glossiness (*The American Heritage Dictionary*, 4th ed.). Glass differs from an opaque object in its ability to reflect or transmit light. Various methods to detect vitreousness of durum wheat kernels have been investigated. Dowell (2000) reported matched classification results between a single−kernel NIR spectroscopy method and human inspectors on obviously vitreous and nonvitreous durum wheat kernels. Sissons et al. (2000) used a commercial single−kernel characterization system (SKCS 4100, Perten Instruments, Springfield, Ill.) to predict semolina mill yield of durum wheat kernels based on vitreousness. As a rapidly developing technology, machine vision has shown great potential for assessing physical properties of grain. Many researchers have combined image acquisition, processing, and analysis techniques with advanced classification algorithms, including statistical analysis and artificial neural network (ANN), to detect grain kernel characteristics, such as color, texture, and various types of damages (Zayas et al., 1994; Luo et al., 1999; Ruan et al., 2001; Bacci et al., 2002). Symons et al. (2003) developed a machine−vision based system to classify durum wheat kernels according to the degree of vitreousness. Their results were highly consistent with those from human inspection. In a previous study, neural−network models were developed based on reflected kernel images to determine the vitreousness of durum wheat using a real−time, image−based wheat quality inspection machine, the GrainCheck 310 (FOSS Tecator, Höganäs, Sweden). The correct classification for vitreousness kernels reached 85% to 90% (Wang et al., 2003).

A common−sense perception of vitreous kernels is that they would allow much more light to transmit than would non−vitreous kernels. Thus, images of kernels taken with transmitted light may carry more information on kernel vitreousness than reflected kernel images. This study was based on this common−sense perception. The objective of this study was to compare the effectiveness of transmitted and reflected kernel images in determining vitreousness.

MATERIALS AND PROCEDURES

SAMPLE PREPARATION

The Grain Inspection, Packers, and Stockyards Administration (GIPSA) of USDA provided test samples for this

Article was submitted for review in September 2003; approved for publication by the Food & Process Engineering Institute Division of ASAE in October 2004. Presented at the 2003 ASAE Annual Meeting as Paper No. 033138.

The authors are **Ning Wang, ASAE Member Engineer,** Assistant Professor, Department of Bioresource Engineering, McGill University−Macdonald Campus, Ste−Anne−de−Bellevue, Quebec, Canada; **Naiqian Zhang, ASAE Member Engineer,** Professor, Department of Biological and Agricultural Engineering, Kansas State University, Manhattan, Kansas; **Floyd E. Dowell, ASAE Member Engineer,** Research Engineer, and **Tom Pearson, ASAE Member Engineer,** Agricultural Engineer, USDA−ARS Grain Marketing and Production Research Center, Kansas State University, Manhattan, Kansas. **Corresponding author:** Ning Wang, MSI−027, Department of Bioresource Engineering, McGill University−Macdonald Campus, 21,111 Lakeshore Ave., Ste−Anne−de−Bellevue, Quebec, Canada H9X 3V9; phone: 514−398−7781; fax: 514−398−8387; e−mail: ning.wang@mcgill.ca.

study. The samples were classified as "hard vitreous and of amber color" (HVAC) or "not hard vitreous and of amber color" (NHVAC) by visual inspection of the Board of Appeals and Review (BAR). A subclass of HVAC, "clean durum kernels inspected as HVAC"; a subclass of NHVAC, "clean durum kernels inspected as NHVAC"; and a subclass of NHVAC, "mottled/chalky durum kernels inspected as NHVAC" (mottled), were used for the tests. Sample of each class weighed 100 g. Before the experiment, 500 kernels were randomly selected from each class to be used as the calibration sample set. Five hundred kernels also were randomly selected from each class to form a validation sample set. The calibration set was used to train ANN models, whereas the validation set was used to test the model performance.

Image Acquisition

Three images were taken for each kernel: a reflected image, a side−transmitted image, and a transmitted image. The reflected and side−transmitted images were taken using a commercial, image−based grain−inspection system in real−time (FOSS Tecator, Höganäs, Sweden). The system uses a CMOS camera to take reflective images with a resolution of 640 × 480 pixels/image and 24 bits of color. The distance between the camera and the kernel was 10 cm. For the reflected images, two 24 LED panels were used to provide white light illumination. Each LED on the panel has a diameter of 5 mm and a view angle of 45° (fig. 1a). The side−transmitted images were taken with two 3 mm, red LEDs positioned at two ends of a cavity in which the kernel was placed. These LEDs have a peak response at 660 nm and a view angle of 100°. The camera used for the side−transmitted images was the same as the one used for the reflected images. The distance between the camera and the kernel was also 10 cm (fig. 1b).

The transmitted images were obtained using a back−light image acquisition system (fig. 1c). The kernel was hand−placed on a glass surface. Incandescent light was placed underneath the glass and was directed upwards. The camera was a simple, board−level CCD camera with a spatial resolution of 640 × 480 pixels. A distance of 12.5 cm between the camera and the kernels was used to provide the best kernel coverage. Examples of reflected, side−transmitted, and transmitted images for HVAC, NHVAC, and mottled kernels are shown in figure 2.

Feature Extraction

Four global features and two types of distribution features, each containing 50 elements, were extracted from each kernel image. Thus, the total number of features used as the inputs to the ANN classification model was 104. The four global features were: (1) sum of the number of rows and the number of columns of the image containing the kernel, (2) sum of sin(hue) of all pixels in the image, (3) sum of cos(hue) of all pixels in the image, and (4) average intensity of the image. These features were developed in a previous study of wheat kernel vitreousness (Wang et al., 2003). They contained both color and spatial information of the kernel images. The simultaneous use of sin(hue) and cos(hue) allowed the quadrant, in which the hue angle was located, to be distinctly defined. For example, a sin(hue) value of 0.707 gives two possible hue values: 45° and 135°. If the cos(hue) value is known to be −0.707, then the hue value can then be determined as 135°.

The 100 distribution features came from two histograms for each image. The first is the histogram for intensity. The intensity range between 50 and 255 was evenly divided into 50 intervals. The numbers of pixels with intensity values falling into each interval were used as the distribution

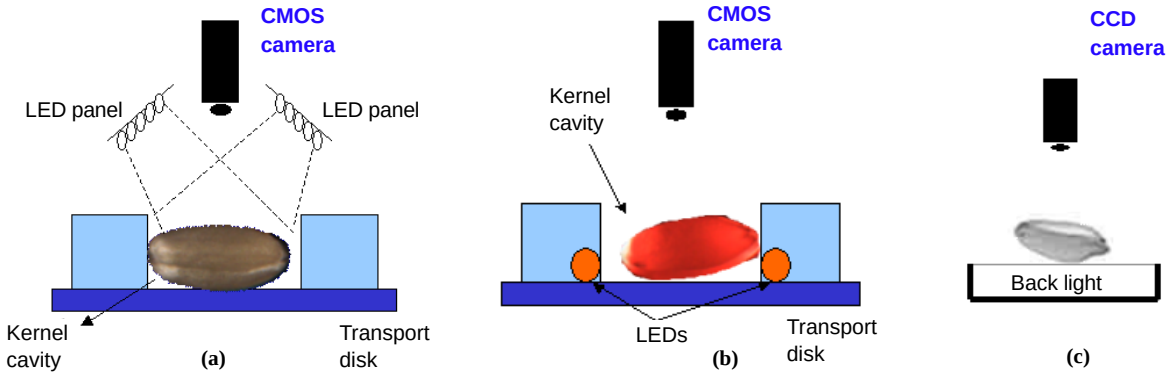

Figure 1. Image acquisition systems for (a) reflected images, (b) side−transmitted images, and (c) transmitted images.

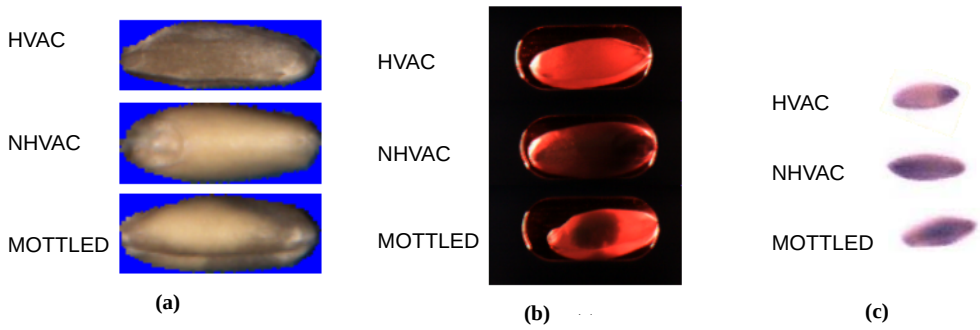

Figure 2. Images of HVAC, NHVAC, and mottled kernels: (a) reflected, (b) side−transmitted, and (c) transmitted.

features. Similarly, the histogram for hue of the same image was used to produce the other 50 features. The 50 equal intervals were derived from the entire range of hue − from 0 to 2π.

Artificial Neural Network (ANN)

A back−propagation network architecture was used in this study (fig. 3). The 104 features extracted from each image were the inputs of the ANN, whereas the number of outputs was equal to the number of classes to be classified. In the network, nodes on adjacent layers are fully connected with weights. These weights were adapted through calibration of the training data in a stepwise manner by repeatedly presenting the data to the ANN for a number of epochs so as to minimize the classification errors. Once the weights were determined, the ANN could be used to categorize samples that were not included in the calibration process. The ANN was designed, trained, and tested using the MATLAB Neural Networks Toolbox (The MathWorks, Inc., Natick, Mass.).

One hidden layer was used in the network. Hidden layers of 10, 20, 50, 75, and 100 nodes were tested, and a 20−node hidden layer was selected through comparison. The basic learning rate used for training was 0.01. The momentum used in training was 0.1, which allowed the changes made to the weights during the previous epoch to be partially incorporated in the current epoch. The input signals were scaled to the interval between −1.0 and 1.0. The activation function used was the sigmoid function. The classification rate for each specific type of kernels was defined as the percentage of this type of kernels (as labeled by BAR) that was correctly classified into the same type by an ANN model.

Experimental Design

Two sets of experiments were conducted. Both were intended to compare the effectiveness of three calibration models developed using images acquired under different illumination conditions (reflected, side−transmitted, and transmitted) in classifying vitreous from non−vitreous kernels. The only difference between the two experiments was that, for experiment 1, samples of only two classes (HVAC and NHVAC) were used, whereas for experiment 2, mottled kernels were used as a part of non−vitreous kernels (NHVAC class) in both calibration and validation.

Experiment 1

Five hundred images taken from each of the HVAC and NHVAC samples were used to establish ANN calibration models. As mentioned earlier, 104 features were used as inputs to the ANN. Two classes (HVAC and NHVAC) were the output of the ANN. The classification results were compared among the models established using three types of images (reflected, side−transmitted, and transmitted). The numbers of kernel images used for validation were the same.

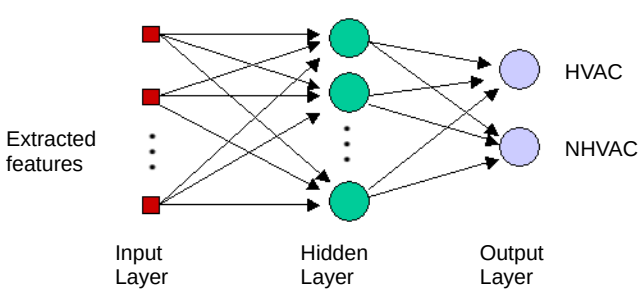

Figure 3. Structure of the ANN.

Experiment 2

Experiment 2 was set up to evaluate the effect of three imaging methods on the classification of mottled kernels. Mottling is a small, non−vitreous area within a kernel. Thus, mottled kernels are considered a subclass of non−vitreous wheat kernels. Because a considerable proportion of non−vitreous kernels are actually mottled, correctly classifying mottled kernels as non−vitreous would greatly improve the overall classification rate of non−vitreous kernels.

Experiment 2 used the same 500 images of HVAC kernels for calibration. For the NHVAC class, only 250 samples were randomly selected from the 500 kernels used in experiment 1. Added to the NHVAC sample were 250 images of randomly selected mottled kernels. Identical numbers of kernels were used in the validation. The 104 features were again used as the inputs to the ANN. Two classes (HVAC and NHVAC) were defined as the outputs of the ANN. The mottled kernels were not defined as an independent output class of the network because they were only considered as a subclass of non−vitreous kernels, and they were not of particular interest to the inspection as long as they can be classified as non−vitreous. Thus, the classification rate for the mottled class was defined as the number of mottled kernels classified into the NHVAC class divided by the total number of mottled kernels. Classification results were again compared among the models established using three types of images (reflected, side−transmitted, and transmitted).

Results and Discussion

Experiment 1

Calibration results of the prediction models using reflected, side−transmitted, and transmitted images showed quite similar classification rates (table 1) for the vitreous and non−vitreous kernels. Table 2 shows the validation results using the validation data set. The model based on transmitted images provided perfect classifications for both HVAC and NHVAC classes. The model using side−transmitted images had higher classification rates for HVAC and NHVAC (97.3% and 85.1%, respectively), compared with those (93.8% and 80.3%, respectively) from the model using reflected images.

Experiment 2

For the calibration data set, the models established using the reflected and side−transmitted images had similar

Table 1. Calibration results for experiment 1.

	Classification Rate (%)	
Prediction model using:	HVAC	NHVAC
Reflected image	100	100
Side−transmitted image	100	98.5
Transmitted image	100	100

Table 2. Validation results for experiment 1.

	Classification Rate (%)	
Prediction model using:	HVAC	NHVAC
Reflected images	93.8	80.3
Side−transmitted images	97.3	85.1
Transmitted images	100	100

performance. The model using the transmitted images, on the other hand, had perfect classifications for both vitreous and non−vitreous (including mottled kernels) classes (table 3). The prediction models were also validated using the validation image set of HVAC, NHVAC, and mottled classes. Table 4 shows the validation results. The models based on transmitted images showed an apparent improvement on the classification of mottled and NHVAC classes. When reflected images were used, only 63% of the mottled kernels were classified as NHVAC. When side−transmitted images were used, the classification rate improved to 83.3%. It was further improved to 92.9% when the transmitted images were used. Meanwhile, the classification rate for the NHVAC class was also improved from 82% to 94.3% for the side−transmitted images and to 100% for the transmitted images. Apparently, the effect of kernel orientation on classification for mottled kernels was largely eliminated with the transmitted image setup.

For most mottled kernels, mottling occurs only on a portion of the kernel, and other areas on the same kernel may appear vitreous. Due to the randomness in orientation when kernels are placed in front of the camera, mottled areas may not always be exposed to the camera's field of view. When images taken were of the reflected type, a considerable fraction of mottled kernels were viewed by the camera as vitreous kernels. Transmitted illumination, on the other hand, allows measurement of the amount of light passing through the kernel. Thus, the effect of kernel orientation imposes a lesser problem for identification of mottled kernels using transmitted images.

Results from the two experiments showed that the types of images used to train ANN models did not have a significant effect on the classification rate for the HVAC class. The use of transmitted illumination mainly improved classification of the NHVAC class, including the mottled class. With the advantages of transmitted images, further study can be conducted to reduce the image features used (probably completely remove the spatial features) and to simplify the algorithm in the classification models. A simpler statistical analysis algorithm that requires a smaller amount of computation, such as discriminant analysis, may be used for faster classification. Furthermore, the transmitted image method would allow use of a simple, low−cost camera with low spatial and color resolutions, such as the one used in this study. This would greatly reduce the cost for both hardware and software of the inspection system.

Summary

Three types of kernel images (reflected, side−transmitted, and transmitted) were collected using two image acquisition systems, and 104 features were extracted from the images. The features were used as the inputs for an artificial neural network, which classified the kernels into two classes: HVAC and NHVAC.

Two experiments were conducted to compare the effectiveness of the ANN models established using three types of images (reflected, side−transmitted, and transmitted). In the first experiment, only HVAC and NHVAC samples were used. The validation results showed that the model based on transmitted images provided perfect classifications for both the HVAC and NHVAC classes. The model using side−transmitted images provided better classification rates than the models using reflected images.

Table 3. Calibration results for experiment 2.

	Classification Rate (%)	
Prediction model using:	HVAC	NHVAC + Mottled
Reflected image	94.7	89.5
Side−transmitted image	94.7	92.2
Transmitted image	100	100

Table 4. Validation results for experiment 2.

	Classification Rate (%)		
Prediction model using:	HVAC	NHVAC	Mottled
Reflected images	88.0	82.0	63.3
Side−transmitted images	87.4	94.3	83.3
Transmitted images	91.6	100	92.9

In the second experiment, mottled samples were added to the NHVAC class to train the ANN models. Output classes of the ANN were still HVAC and NHVAC. The validation results indicated a great improvement in classifying the molted kernels using transmitted illumination. The classification rates for mottled kernels using transmitted images reached 92.9%, compared to 83.3% using side−transmitted images and 63.3% using reflected images. On the other hand, use of transmitted illumination did not show significant impact on classification of the HVAC kernels.

Results of the study also indicated that using transmitted illumination may greatly reduce hardware and software requirements for the inspection system, while providing faster and more accurate results for inspection of vitreousness of durum wheat.

References

Abaye, A. O., D. E. Brann, M. M. Alley, and C. A. Griffey. 1997. *Winter Durum Wheat: Do We Have All the Answers?* Pub. No. 424−802. Blacksburg, Va.: Virginia Tech, Virginia Cooperative Extension.

Bacci, L., B. Rapi, F. Colucci, and P. Novaro. 2002. Durum wheat quality evaluation software. In *Proc. World Congress of Computers in Agriculture and Natural Resources*, 49−55. St. Joseph, Mich.: ASAE.

Dowell, F. E. 2000. Differentiating vitreous and nonvitreous durum wheat kernels by using near−infrared spectroscopy. *Cereal Chemistry* 77(2): 155−158.

Luo, X., D. S. Jayas, and S. J. Symons. 1999. Identification of damaged kernels in wheat using a color machine vision system. *J. Cereal Science* 30(1): 49−59.

Ruan, R., S. Ning, L. Luo, P. Chen, R. Jones, W. Wilcke, and V. Morey. 2001. Estimation of weight percentage of scabby wheat kernels using an automatic machine vision and neural network based system. *Trans. ASAE* 44(4): 983−988.

Sissons, M. J., B. G. Osborne, R. A. Hare, S. A. Sissons, and R. Jackson. 2000. Application of the single−kernel characterization system to durum wheat testing and quality prediction. *Cereal Chemistry* 77(2): 4−10.

Symons, S. J., L. Van Schepdael, and J. E. Dexter. 2003. Measurement of hard vitreous kernels in durum wheat by machine vision. *Cereal Chemistry* 80(5): 511−517.

Wang, N., F. E. Dowell, and N. Zhang. 2003. Determining wheat vitreousness using image processing and a neural network. *Trans. ASAE*. 46(4): 1143−1150.

Zayas, I. Y, D. B. Bechtel, J. D. Wilson, and E. E. Dempster. 1994. Distinguishing selected hard and soft red winter wheat by image analysis of starch granules. *Cereal Chemistry* 71(1): 82−86.